Case Studies in Thermal Engineering 69 (2025) 106023

Contents lists available at ScienceDirect

Case Studies in Thermal Engineering

journal homepage: www.elsevier.com/locate/csite

Experimental study on the optimization of thermal environment and airflow organization in a ventilated underground refuge chamber using deflectors

Hang Jin [a], Zujing Zhang [a,*], Ruiyong Mao [a], Jiri Zhou [b], Hongwei Wu [c], Xing Liang [d]

[a] College of Civil Engineering, Guizhou Provincial Key Laboratory of Rock and Soil Mechanics and Engineering Safety, State Key Laboratory of Public Big Data, Guizhou University, Guiyang, 550025, China
[b] China MCC5 Group CORP.LTD., MCC5 Tower, No. 9 Wuye Road, Jinjiang District, Chengdu, 610000, China
[c] School of Physic, Engineering and computer science, University of Hertfordshire, Hatfield, AL10 9AB, United Kingdom
[d] School of Computer Science and Mathematics, Kingston University London, KT1 2EE, United Kingdom

ARTICLE INFO

Keywords:
Underground refuge chamber
Mechanical ventilation
Deflectors
Ambient temperature
Airflow organization

ABSTRACT

Acceptable temperature is crucial for underground refuge chamber (URC) to ensure the safety and comfort of occupants. A novel temperature control scheme combining mechanical ventilation with deflectors was proposed for URCs. In this study, the effects of ventilation rate (VR), deflector height and deflector angle on ambient temperature control performance and airflow organization of URC were investigated through orthogonal experiments. Results show that: (I) The ambient temperature gradient of URC decreases with the increase of VR and deflector height. (II) With VR of 350 m^3/h, deflector height of 1.40 m, and deflector angle of 0°, compared to the situation without deflectors, the temperature unevenness coefficient can be effectively reduced, the head-to-foot temperature difference can meet the design standard requirements, the waste heat emissions efficiency is increased by 46.1 %, and an average decrease in ambient temperature of 2 °C (III) The influence of various factors on the ambient temperature control performance in the URC is as follows: deflector height > VR > deflector angle.

Nomenclature

σ	Standard deviation	E_T	Efficiency of waste heat emissions
N	The number of sample data	K_t	Temperature unevenness coefficient
μ	Average value of the sample data.	t_i	Temperature of the measurement points
H	Height of measurement point, m	H_d	Height of deflector, m
Q	Dependent variable	***Acronyms***	
x	Independent variable	URC	Underground refuge chamber
n	Number of measurement points	VR	Ventilation rate, m^3/h
$\bar{t}$	Average temperature of the measurement points, °C	RH	Relative humidity, %
		PCC	Phase change chairs
Δt	Temperature differences, °C	PCP	Phase change panels
Subscripts		TIC	Thermal insulation and cooling

(*continued on next page*)

* Corresponding author.
E-mail address: zjzhang3@gzu.edu.cn (Z. Zhang).

https://doi.org/10.1016/j.csite.2025.106023
Received 2 December 2024; Received in revised form 14 February 2025; Accepted 10 March 2025
Available online 11 March 2025

(*continued*)

σ	Standard deviation	E_T	Efficiency of waste heat emissions
x_i	Value of the sample data	PVC	Polyvinyl chloride
σ_Q	Uncertainty of the dependent variable	VT	Ventilation temperature, °C
σ_x	Uncertainty of the independent variable	FS	Front section
T_{in}	Inlet temperature, °C	MS	Middle section
T_{out}	Outlet temperature, °C	BS	Back section
T_w	Ambient temperature, °C		

1. Introduction

Urbanization is an important process in human society in the 21st century [1–3]. Currently, the buildings on the ground are becoming increasingly saturated, and the contradiction between urban development and land scarcity is prominent. Developing underground space has become a necessary path for the sustainable development of urbanization [4–7]. However, due to the challenges of constructing underground buildings that provide suitable living and working environments, there are still many issues that need to be addressed. The environmental parameters of the underground space are directly related to the living experience and comfort level of the occupants [8,9]. In particular, the closed environment of underground buildings often faces the hazards of high humidity and high heat. Personnel who are exposed to such conditions for a long time may experience adverse effects in terms of subjective perception, psychology, and physiological behavior [10–13]. Therefore, it is especially crucial to propose effective improvement measures to address the adverse effects brought about by underground thermal hazards.

As a typical underground artificial structure, the URC serves as an emergency place for miners to find safety during disasters in coal mines [14–16]. After entering the URC, miners may need to stay for a long time waiting for rescue. The continuous metabolic heat dissipation of personnel and the humid and hot environment of the underground confinement can deteriorate the thermal environment inside the refuge chamber, which has increasingly attracted the attention of scholars in environmental control technology.

Domestic and foreign scholars have proposed different cooling and dehumidification strategies for the thermal hazards caused by high humidity and high temperature. As a cooling measure of traditional refuge chamber, mine air pressure is usually composed of air compressors, gas storage tanks and conveying pipes to send cooling air into the refuge chamber, and use high-speed airflow to drive the surrounding air flow to form ventilation effect [17–19]. The primary objective is to provide fresh air, expel harmful gases and dust, regulate room temperature and humidity, and ensure the safety and well-being of miners. Phase change cooling is a temperature control measure based on the absorption of heat by a substance during its phase change process, which in turn affects the surrounding environmental temperature [20,21]. In recent years, it has also been increasingly applied in temperature control strategies for URC. Li et al. [22] explored the influence of different layout of phase change plates on indoor temperature control in an URC, finding that arranging three rows of phase change plates (PCP) is more beneficial for indoor temperature control. Gao et al. [23–26] proposed a new method of coupled cooling of phase change chair (PCC) and PCP, finding that under natural convection conditions, the temperature control requirements of 96 h can be met in the URC with an initial rock temperature of 23 °C. In addition, as a cooling measure without safety risks, ice storage is often favored by researchers in the temperature control and dehumidification strategy of URC by taking advantage of the high melting latent heat of ice [27,28]. Xu et al. [29] studied the influence of different sizes of ice storage plates on the cooling effect in the URC, and found that when the size of ice storage plates is 0.6 m × 0.32 m × 0.05 m (long × wide × height) and the storage temperature is −10 °C, it is more conducive to temperature regulation. Considering that power failure usually occurs in coal mine disasters, Zhang and Guo et al. [30,31] developed a set of pressure air-ice storage device, and studied the heat exchange performance and dehumidification performance of the ice storage device. They found that the heat exchange performance was optimal at a wind speed of 10 m/s, a temperature of 32 °C, and with 18 heat exchange tubes. The dehumidification efficiency was most affected by the inlet wind speed, with a 12.81 % increase in dehumidification efficiency when the inlet wind speed decreased from 15 m/s to 5 m/s.

However, relying solely on ventilation for cooling requires an excessively large air supply to meet the temperature control requirements of the URC. Although lowering the supply air temperature can reduce the amount of ventilation needed, obtaining low-temperature fresh air also requires energy consumption from the air conditioning system. Phase change cooling and ice storage cooling can meet the temperature control conditions of the URC, but they mostly rely on external energy. The consumption of electrical energy and phase change materials is an important factor that cannot be ignored. In addition, these temperature control and dehumidification measures need to be considered at the beginning of the construction of the URC. For already constructed underground buildings, it is difficult to rebuild a cooling system. To address this issue, it is necessary to propose a cooling strategy that is easy to implement, saves energy consumption and has obvious temperature control effect.

In fact, reasonable air flow organization and uniform air distribution can achieve heat exchange with minimal operating energy consumption, thereby reducing the energy consumption of the cooling system and improving the comfort of indoor personnel [32,33]. Strategies to improve indoor thermal environments by optimizing airflow organization have been involved in many places. Wu and Mao et al. [34,35] optimized airflow organization by arranging barriers in the data center to improve local hotspots generated by servers. Xu et al. [36] proposed a method for optimizing airflow organization by integrating thermal insulation and cooling (TIC) baffles in tunnel excavation, by implementing TIC baffles, the average airflow temperature in the tunnel excavation decreased by 1.5 °C–1.8 °C, saving approximately 5.11 kW of cooling energy. Zhang et al. [37] improved the thermal comfort inside the kitchen by optimizing the air flow distribution in summer, and found that when the air supply angle of the air conditioner was reduced to 45°, the thermal comfort was significantly improved. Previous research has verified the feasibility and importance of airflow management,

therefore optimizing airflow organization within underground structures to improve the indoor thermal environment is worth studying.

In summary, energy consumption is a significant challenge that cannot be ignored in the existing temperature control measures for URCs. On the other hand, these measures often overlook the impact of airflow organization on environmental temperature distribution and the comfort of indoor personnel. Therefore, optimizing airflow distribution through low-energy methods to improve underground thermal environment and comfort is a problem that needs to be addressed. The arrangement of deflectors as an effective method to improve airflow distribution has advantages such as low cost and easy installation, and its working principle mainly relies on inducing airflow direction changes through the pressure difference generated by the physical structure [38,39]. However, there are relatively few studies on the feasibility of applying deflectors to underground buildings and the improvement of underground thermal environment by different layout methods. In this study, the cooling measures of mechanical ventilation and deflectors are proposed to optimize indoor air distribution through different layout methods of deflectors, so as to effectively control the temperature of URC.

In this paper, the deflector is placed at the lower end of the air inlet perpendicular to the horizontal ground direction, and the effects of three key factors, namely the ventilation rate (VR), deflector height and deflector angle, on the thermal environment of the URC are analyzed through orthogonal experiments, and the feasibility of the deflector is verified to be used in the URC for optimizing the organization of the thermal environment, in order to obtain the optimal arrangement of the deflector. The results of this study will provide theoretical guidance for controlling the thermal environment in underground confined spaces.

2. Materials and methods

2.1. Experimental environment and principle

The experiment is carried out in an URC laboratory with a capacity of 30–50 people, as shown in Fig. 1, the main structure of the URC is constructed from C30 concrete with a thermal conductivity of 0.90 W/(m·°C), a density of 1950–2500 kg/m^3, and a specific heat capacity of 970 J/(kg·K), with thicknesses of 0.6 m in the floor, 0.8 m in the roof, and a minimum of 0.55 m in the walls on both sides. The URC laboratory is 12.6 m × 4 m(long × wide). The section of the chamber is an arch with a height of 3 m, a width of 4 m, a vertical wall height of 1.5 m, and a perimeter of 12.35 m.

In order to optimize the airflow organization and improve the comfort of the evacuees in URC, 10 deflectors are placed at the lower end of the air inlet. As shown in Fig. 2 (a), the deflectors are made of polyvinyl chloride (PVC) plastic plate, each of which is 2m × 0.3m × 0.01m(long × wide × height). As shown in Fig. 2 (b), considering that the experimental study is conducted in a simulated underground mine, where the URC is relatively close to the ground and the air quality meets the personnel safety absorption standards, this study does not filter or purify the air. Instead, it directly utilizes fans to draw air from the tunnel to be delivered into the URC. The rated air flow of the fan is 1530 m^3/h, with a power of 1.5 kW, voltage of 380V, total pressure of 2400Pa, and rotational speed of 2800 r/min.

As shown in Fig. 3, the air inlet is 1.8 m from the ground, and the distance between two adjacent air inlets is 0.5 m. The VR of fan is determined by an anemometer. Due to the low density of high temperature exhaust gas, it will be deposited in the upper area of the chamber by the action of thermal buoyancy, so two air outlets are set above the two ends of the chamber, with a diameter circular of 20 cm and a distance of 2.65 m from the ground. As the fresh air continues to enter the indoor part, the indoor air pressure continues to increase, and the polluted air will be discharged through the outlet in time. The continuous supply of fresh air also ensures that some of the energy consumed by the exhausted gas is promptly replenished, thus maintaining a safe and comfortable indoor environment. In order to investigate the airflow organization and human comfort in a 30-person URC, a 100W heating tube with fins is used to simulate human heat dissipation. Human heat is the main source of heat in URC, heat dissipation during evacuation is 120 W [40]. The heating tubes with a length of 35 cm and a profile diameter of 2 cm are distributed in 4 columns × 9 rows, and each heating tube is 50 cm high from the ground. The six temperature measurement points are arranged at three horizontal heights of 0.1, 1.1 and 1.8 m above the ground. Ambient and inlet ventilation temperatures (VT) are measured by PT100 thermocouples calibrated with a 0 °C ice-water mixture. The arrangement of heating tubes, air inlets and measurement points are shown in Fig. 3.

(a) External environment **(b) Internal environment**

Fig. 1. URC experimental environment.

(a) Deflectors (b) Variable frequency fan

Fig. 2. Experimental equipment.

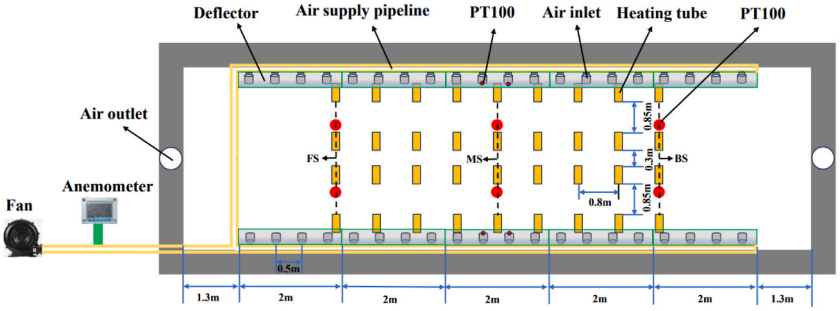

Fig. 3. Layout of the heating tube, air inlet and measuring point.

2.2. Design of experimental cases

This experiment is based on the optimization of air flow organization in URC of human comfort. Due to the fluctuation of experimental ambient temperature in a certain range, the inlet temperature of each group of experimental conditions is different. Therefore, before carrying out each group of experiments, the ambient temperature difference on the experiment day should be ensured as far as possible, and the temperature difference should be less than 2 °C. thereby ensuring that the ventilation temperatures for each set of experiments remained relatively constant. Considering that the per capita air supply of the URC is not less than 0.1 m^3/min [41], the ventilation level of 30 people is set to 250 m^3/h, 300 m^3/h, and 350 m^3/h. According to the height of the head from the ground when sitting, the deflector height is set at three levels: 1.40 m, 1.25 m, and 1.10 m. To change the air intake angle of the inlet, the deflector angle is set at three levels: 0°, 15°, and 30°. The arrangement of the deflector heights and angles is shown in Fig. 4. According to the orthogonal experiment design, the orthogonal test conditions with 3 factors and 3 levels can be obtained as shown in Table 1. Meanwhile, case 10 (VR of 350 m^3/h, without deflector) is set as the blank control group.

2.3. Data acquisition and processing

Data collection instruments include temperature probe PT100, temperature collector and anemometer, separately see Fig. 5(a) and (b) and (c), the detailed parameters of these instruments are listed in Table 2. The data collection time of the temperature collector is set to 2 min. The anemometer is used to monitor the VR. After the VR monitored by the anemometer reaches the value to be set in the experiment, the inlet air volume can be kept constant by stopping the regulation of the frequency converter to keep the fan speed constant.

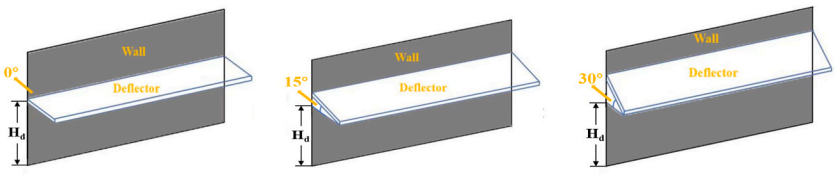

(a) 0° (b) 15° (c) 30°

Fig. 4. Arrangement of deflector heights and angles.

Table 1
Parameters of experimental cases.

Case	VR (m^3/h)	Deflector height (m)	Deflector angle (°)
1	350	1.40	0
2	350	1.25	15
3	350	1.10	30
4	300	1.40	15
5	300	1.25	30
6	300	1.10	0
7	250	1.40	30
8	250	1.25	0
9	250	1.10	15
10	350	–	–

(a) PT100 (b) Temperature collector (c) Anemometer

Fig. 5. Data acquisition instruments.

Table 2
Data acquisition instrument parameter.

Name	Model	Range	Accuracy	Remarks
Thermocouple	PT100	(-50~200) °C	±0.01 °C	/
Temperature collector	JK4000	(-200–1800) °C	0.01 °C	Work environment: (20 % ~ 90 %) RH
Anemometer	LSFS-4	(0–9000) m^3/h	0.02 %	Work environment: (−40–80) °C

In the experimental process, due to the experimental ambient temperature is difficult to constant, VT exists a certain range of fluctuations, which in turn will affect the accuracy of the indoor ambient temperature and the temperature of the air outlet. In order to minimize errors caused by fluctuations in VT, the highest and lowest temperatures at each of the three horizontal heights are excluded, and the average of the remaining data is taken as the ambient temperature at each of the three horizontal heights. The air outlet temperature is taken as the average of two temperature measurement points to improve the accuracy and reliability of the experimental data. Considering that this method is used for data processing in each group of working conditions, this study takes the data at the time point t = 24 h from the blank control group case 10 as an example for deviation calculation. the deviation calculation formula is as follows:

$$\sigma = \sqrt{\frac{1}{N}\sum_{i=1}^{N}(x_i - \mu)^2} \tag{1}$$

Where, σ is the standard deviation; N is the number of sample data; x_i is the value of the sample data; μ is the average value of the sample data.

The blank control group case 10 measured temperatures at 1.8m height at t = 24 h are 29.6, 30.4, 30.6, 30.7, 30.7, and 32.4 °C. The data after removing the maximum and minimum values will be substituted into formula (1) for calculation as follows:

$$\mu = \frac{30.4 + 30.6 + 30.7 + 30.7}{4} = 30.6^{\circ}C$$

$$\sigma_{1.8} = \sqrt{\frac{1}{4} \times \left[(30.4 - 30.6)^2 + (30.6 - 30.6)^2 + (30.7 - 30.6)^2 + (30.7 - 30.6)^2\right]} = 0.122$$

Similarly, at t = 24 h for case 10, the measured temperatures at a height of 1.1m are 27.1, 29.3, 29.4, 29.6, 29.7, and 31.3 °C. At a height of 0.1m, the measured temperatures are 27.8, 28.1, 28.2, 28.8, 28.9, and 29.7 °C. Substituting these values into formula (1), the deviations are:

$\sigma_{1.1} = 0.158$

$\sigma_{0.1} = 0.354$

2.4. Uncertainty analysis

This paper investigates the effect of changing the air inlet angle by setting the deflector in a reasonable position on the temperature control and airflow organization distribution of the chamber, and calculates the uncertainty of this experiment using case 1 as an example. Calculating the uncertainty of the experimental data according to the method proposed by Taner et al. [42]. The relationship between the variable Q and the independent variables x_1, x_2, …, x_n can be expressed as follows:

$$Q = f(x_1, x_2, \ldots, x_n) \tag{2}$$

The uncertainty of the variable Q is as follows:

$$\sigma_Q = \sqrt{\left(\frac{\partial Q}{\partial x_1}\sigma x_1\right)^2 + \left(\frac{\partial Q}{\partial x_2}\sigma x_2\right)^2 + \cdots + \left(\frac{\partial Q}{\partial x_n}\sigma x_n\right)^2} \tag{3}$$

Here σx_1, σx_2, …, σx_n are the uncertainties of x_1, x_2, …, x_n respectively.

Table 3 shows the uncertainties of the measured and calculated parameters.

2.5. Experimental procedure

The key steps of the experiment are as follows.

(1) Check the reliability of the system one day before the experiment, adjust the height and angle of the deflector plate required by each group of working conditions to ensure the temperature measurement point and the heating tubes can operate normally, and the temperature collector can record data automatically.
(2) Before the work of the heating tubes, the tester enters the laboratory and measures the initial wall temperature with an infrared thermometer, taking three measurement points on each wall to ensure that the initial average wall temperature of each group of experimental conditions is 21.5 °C.
(3) Close the laboratory door, switch on the temperature collector and measure the average initial temperature of the chamber environment to be 21.0–21.5 °C.
(4) Simultaneous switching on of fans and heating tubes, continuous operation for 24h.
(5) Repeat the above experimental procedure to complete all experimental conditions.
(6) End the experiment, turn off the heater and fan, and save the experimental data.

3. Results

3.1. Temperature variations in different locations of the URC under ventilation

To investigate the temperature variation at different positions in the chamber under pure ventilation conditions, the blank control group case 10 is selected for analysis. The temperature distribution at different heights inside the chamber is shown in Fig. 6 (a). It can be seen that at the same time node, the temperature distribution increases with increasing height. This is due to the presence of indoor heat sources, where the air is heated and buoyancy forces cause the high-temperature air to move towards the upper area of the chamber, while the low-temperature air sinks towards the lower area of the chamber, resulting in a significant temperature stratification in the URC. The average temperature of the three sections of the chamber over time is shown in Fig. 6 (b). It can be seen that the highest ambient temperature is at the MS of the chamber, followed by the BS, and the FS has the lowest ambient temperature. Due to the heat radiation at both ends of the MS of the chamber, heat dissipation from the human body is concentrated, and the high-

Table 3
Uncertainties of measured and calculated parameters.

Items	Units	Uncertainty
Measurement parameters		
Inlet temperature	°C	0.5 %
Outlet temperature	°C	0.5 %
Ambient temperature	°C	0.5 %
Ventilation rate	m^3/h	0.02 %
Calculate parameters		
Head-to-foot temperature difference	°C	0.71 %
Efficiency of waste heat emissions		0.61 %
Temperature unevenness coefficient		0.12 %

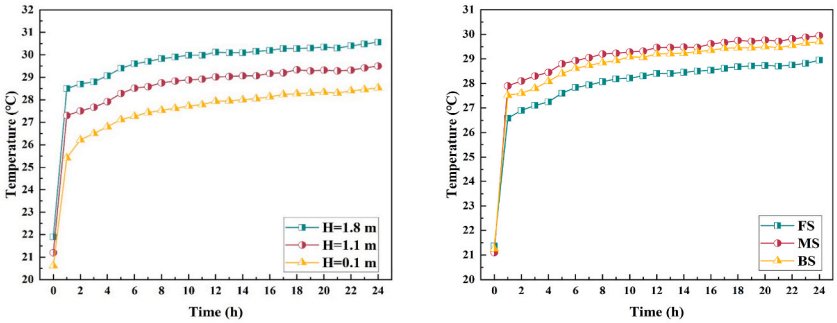

Fig. 6. Temperature changes over time at different locations.

temperature air could not be quickly discharged outside, leading to heat accumulation and relatively higher temperature compared to the FS and BS. Although both the FS and BS of the chamber are close to the air outlet, the supply air duct passes through the FS before reaching the BS, resulting in some loss and delay of fresh air reaching the BS of the chamber, causing the ambient temperature at the BS to be higher than that at the FS.

3.2. Sensitivity analysis

3.2.1. Effect of VR

Under the condition of constant height and angle of the deflector, the influence of different VRs on ambient temperature in the chamber is shown in Fig. 7. When the VRs are 350, 300, and 250 m^3/h, the temperature in the URC rapidly rises from the initial 21.1 °C to around 26.5 °C within 1 h. Subsequently, the temperature slowly increases over time, and after 24 h, the ambient temperatures are controlled at 29.0, 29.3, and 29.3 °C, with average temperature rise rates of 0.329, 0.342, and 0.342 °C/h, respectively. Overall, the ambient temperature gradient in the URC decreases as the VR increases. This is because with a higher VR, the incoming air speed is also higher, which accelerates the heat exchange rate between the indoor cold and hot air, resulting in better temperature control performance in the chamber environment.

3.2.2. Effect of deflector height

Under the condition of constant VR and deflector angle, the influence of different deflector height on ambient temperature in the chamber is shown in Fig. 8. When the deflector heights are 1.40, 1.25, and 1.10 m, the ambient temperature in the URC rapidly increases from the initial 21.2 to 25.8, 26.9, and 27.3 °C within 1 h, and then gradually rises over time. After 24 h, the temperatures are controlled at 28.9, 29.2, and 29.5 °C, with average temperature rise rates of 0.321, 0.333, and 0.346 °C/h, respectively. The temperature gradient in the URC decreases with the increase of deflector height. At the same time point, the URC with a deflector height of 1.40 m has the lowest ambient temperature, followed by 1.25 m and 1.10 m deflector heights. This is because after installing the deflectors in the URC, the fresh air perpendicular to the ground will first collide with the deflector, forming an air lake similar to

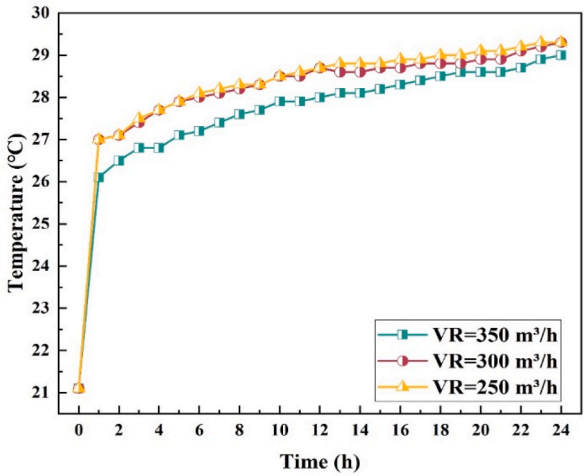

Fig. 7. Ambient temperature varies with time under different VR.

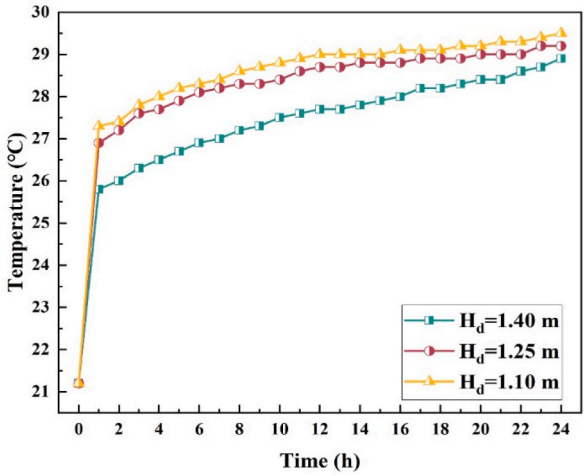

Fig. 8. Ambient temperature varies with time under different deflector heights.

displacement ventilation. The impact of deflector height variation on indoor airflow organization is mainly reflected in the height of the air lake formation. When the deflector height is higher, it is closer to the air inlet, and the airflow will spread along the direction of the deflector arrangement after hitting the deflector, resulting in a slight increase in the velocity of the cold airflow and accelerated heat exchange at the deflector height. As mentioned in section 3.1, the temperature in the upper area of the URC is higher. Therefore, with the increase of deflector height, the temperature distribution in the URC becomes more uniform in height, effectively reducing the ambient temperature.

3.2.3. Effect of deflector angle

Under the condition of constant VR and deflector height, the influence of different deflector angles on ambient temperature in the chamber is shown in Fig. 9. When the deflector angles are 0°, 15° and 30°, the ambient temperature in the URC rapidly increases from the initial 21.2 to 26.3, 26.9 and 26.8 °C within 1 h, and then gradually rises over time. After 24 h, the temperatures are controlled at 29.2, 29.4 and 29.3 °C, with average temperature rise rates of 0.333, 0.342 and 0.338 °C/h, respectively. At the same time point, the chamber ambient temperature with a deflector angle of 0° is generally lower than that with deflector angles of 15° and 30°. This is because when the deflector is arranged horizontally, the airflow disturbance increases after passing through the deflector, enhancing the turbulence of the newly introduced cold airflow, increasing the heat exchange in the upper space of the chamber for a certain period of time, leading to a decrease in the average temperature inside the chamber. In addition, after the cold air is obstructed by the horizontal baffle, most of it moves on the upper wall of the deflector, with a higher density of colder fresh air, which then descends, further lowering the temperature in the space. When the deflector angle is 15° and 30°, due to the angle of inclination between the deflector and the horizontal plane, a portion of the airflow will spread along the direction of the inclined deflector upon colliding with it. Therefore, the heat transfer of cold and hot air in the area above the deflector is slowed down, resulting in higher temperature in the

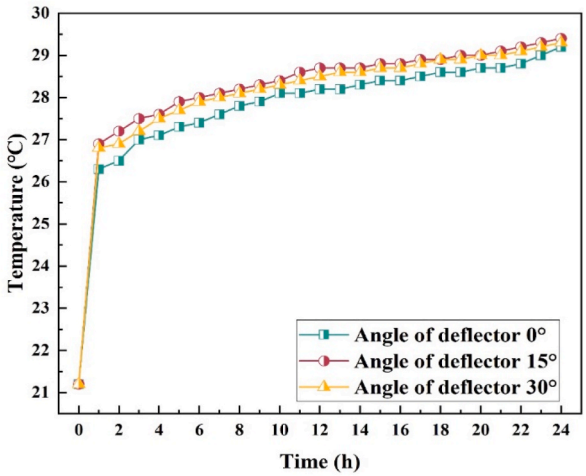

Fig. 9. Ambient temperature varies with time under different deflector angles.

upper part of the chamber, lower temperature in the lower part, disordered temperature distribution in the height, and relatively poor temperature control effect in the chamber. In conclusion, the arrangement of horizontal deflector can to some extent improve the uniformity of indoor temperature and is better than the other two arrangement angles.

3.3. URC airflow organization evaluation

3.3.1. Temperature unevenness coefficient

The uniformity of the airflow organization within an URC has a significant impact on the comfort experienced by the evacuees, and for this reason the temperature unevenness coefficient [43,44] is used to evaluate the airflow organization of URC. In order to investigate the temperature unevenness coefficient in a 30-person URC, 18 temperature measurement points are arranged uniformly in the chamber at three horizontal heights of 0.1, 1.1 and 1.8 m, and the temperature values are extracted and processed for each group of experimental conditions, the temperature unevenness coefficient K_t is calculated by using Eq. (4).

$$K_t = \frac{\sqrt{\frac{1}{n}\sum (t_i - \bar{t})^2}}{\bar{t}} \tag{4}$$

Where n is the number of measurement points, t_i is the temperature of the measurement points, $\bar{t}$ is the average temperature of the measurement points, the smaller the value of K_t, the better the uniformity of airflow distribution and the better human comfort experience.

The temperature unevenness coefficient at the head height in standing (1.8 m), head height in sitting (1.1 m), and ankle height (0.1 m) in 10 experimental conditions are shown in Fig. 10. At the height of 1.1 m, the temperature unevenness coefficient fluctuates greatly, and its value is significantly higher than that of the temperature unevenness coefficient at the height of 1.8 m and 0.1 m. It can be shown that the uniformity of airflow distribution at 1.8 m and 0.1 m height is better than that at 1.1 m height. In case 10 (without deflector), the temperature unevenness coefficients at heights of 0.1, 1.1, and 1.8 m are 0.0254, 0.0446, and 0.0224, respectively. In case1-9 (with deflector), case 1 and case 5 are significantly lower than in other cases at the height of 1.1 m with high temperature unevenness coefficient. The temperature unevenness coefficients of case 1 and case 5 at the 1.1m height plane are 0.0342 and 0.0335, respectively, which are 23.32 % and 24.88 % lower than case 10. This indicates that with the same VR, setting up deflectors in the URC at appropriate heights and angles can effectively improve the indoor airflow organization distribution characteristics, enhance the uniformity of flow field distribution, and better meet the requirements of human comfort experience. Considering the temperature unevenness coefficient values at the three heights, case 1 and case 5 are selected as the better operating conditions.

3.3.2. Head-to-foot temperature difference

The head-to-foot temperature difference in the rest area is a measure of human comfort experience and an important indicator of air quality evaluation [45]. The head of the evacuee is separately set to be 1.8 m and 1.1 m above the ground for standing and sitting, and the ankle of the evacuee is set to be 0.1 m above the ground. In order to meet the requirements for comfort in the rest areas and to ensure the indoor air quality of the URC, the following standards should be fulfilled:

Standing head-to-foot temperature difference [45]:

$$\Delta t_{1.8-0.1} \leq 3°C \tag{5}$$

Sitting head-to-foot temperature difference [45]:

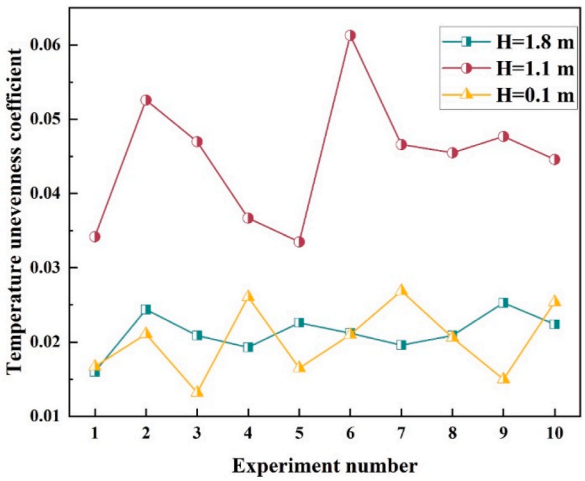

Fig. 10. Variation of temperature unevenness coefficient at three heights.

$$\Delta t_{1.1-0.1} \leq 2°C \tag{6}$$

The trend of head-to-foot temperature difference with time for 10 groups of experimental conditions is shown in Fig. 11. The red dotted line in Fig. 11 (a) represents the design standard requirement of head-to-foot temperature difference when the human is standing, and the purple dotted line in Fig. 11 (b) represents the design standard requirement of head-to-foot temperature difference when the human is sitting. It can be seen that 10 groups of conditions to meet the standard requirements of head-to-foot temperature difference is only case 1, the remaining 9 groups of conditions in the beginning of the experiment in the 0–2 h, standing and sitting head-to-foot temperature difference are not to meet the standard requirements. The temperature difference between head and foot in the standing position increased steeply from about 1 °C initially to about 3.5 °C, and the temperature difference between head and foot in the sitting position increased steeply from about 0.5 °C to about 2.5 °C, the temperature difference gradually decreases after 2 h, and the temperature difference between the head and foot of the vast majority of working conditions after 2 h also meets the design standard requirements. This may be due to the fact that during the first 2 h of the experiment, the human dissipates heat at the fastest rate and the ambient temperature of the refuge rises the fastest. Due to the presence of a heat source, the cold air is heated by the heat source and then moves towards the upper part of the refuge by thermal buoyancy, resulting in the ambient temperature above the refuge rising at a much faster rate than that below it, and the difference between the ambient temperatures is increased. Comparing case 1 and case 10, the standing and sitting head-to-foot temperature difference of case 10 do not meet the design criteria in the first 2 h when the VR is 350 m^3/h for both cases. The installation of a suitable deflector improves the uniform distribution of airflow in the chamber, which helps to improve the comfort of the evacuees in the URC.

3.3.3. Efficiency of waste heat emissions

Efficiency of waste heat emissions [46,47] is an indicator of the ability to remove excess heat from a room by introducing fresh air into the room, and can also be referred to as temperature efficiency (E_T). This is determined by the inlet temperature (T_{in}), the outlet temperature (T_{out}), and the ambient temperature of the URC (T_w). The calculation formula is as follows:

$$E_T = \frac{T_{out} - T_{in}}{T_w - T_{in}} \tag{7}$$

Since the T_{in} is affected by the ambient temperature, in conducting each group of experiments, a time was chosen when weather conditions are approximately the same to carry out, the atmospheric temperature fluctuates from 18 °C to 27 °C, and the difference of the air supply temperature is within 2 °C. Although E_T is a performance parameter that is directly determined by the temperature value, it can visually reflect the ability of the indoor ventilation of a refuge to remove excessive heat, and is one of the most important indicators for air quality evaluation.

The average efficiency of waste heat emissions for the 10 sets of experimental conditions is shown in Table 4. It can be seen that case 1 has the highest efficiency due to the fact that even though the outlet temperature is the lowest, the ambient temperature of the chamber is also the lowest, and the ambient temperature of the chamber affects the efficiency of waste heat emissions more than the temperature of the inlet. Compared with the efficiency of waste heat emissions of 1.93 for case 10, the efficiency of waste heat emissions of case 1 is improved by 46.1 % with the same amount of VR. Eq. (5) shows that, for a given inlet temperature and outlet temperature, the ambient temperature of the refuge is sufficiently low to improve the efficiency of the refuge's waste heat emissions, and the comfort of the evacuees is significantly improved.

3.4. Analysis of orthogonal test result

In order to determine the influence of three factors, namely VR, deflector height, and deflector angle, on the control performance of the ambient temperature in an URC with 30 people continuously dissipating heat for 24 h, the optimal layout scheme of the URC facilities can be obtained through orthogonal experimental results. From Table 5, it can be seen that the ranges corresponding to the three influencing factors of VR, deflector height, and deflector angle are 0.26, 0.63, and 0.10, respectively. The ranking of the influences of the three factors on the control of the ambient temperature in the URC is: deflector height > VR > deflector angle. Meanwhile, through the range analysis, the optimal layout scheme of indoor facilities is case 1, that is, when deflector height is 1.40 m, VR is 350 m^3/h, and deflector angle is 0°.

4. Discussion

4.1. Comparison of temperature control performance

The results section shows that the arrangement of the deflectors has a significant impact on the organization of airflow and ambient temperature. Based on the orthogonal experimental results, it can be concluded that the optimal arrangement for the URC is case 1, with a VR of 360 m^3/h, a deflector height of 1.40 m, and a deflector angle of 0°.

Comparison of average environmental temperature between Case1 and blank control group Case10 in the refuge chamber is shown in Fig. 12. The VT of the two experimental conditions varies with the ambient temperature. The VT of case 1 fluctuates from 20.8 °C to 25.7 °C, with an average supply air temperature of 23.7 °C. The VT of case 10 fluctuates from 22.3 °C to 25.4 °C, with an average supply air temperature of 23.9 °C. At 1 h, the ambient temperature of case1 rises from the initial 21.1 °C–24.4 °C, while case10 rapidly rises from 21.2 °C to 27.3 °C, resulting in a maximum temperature difference of 2.9 °C between the two conditions. From 2 to 24 h, the

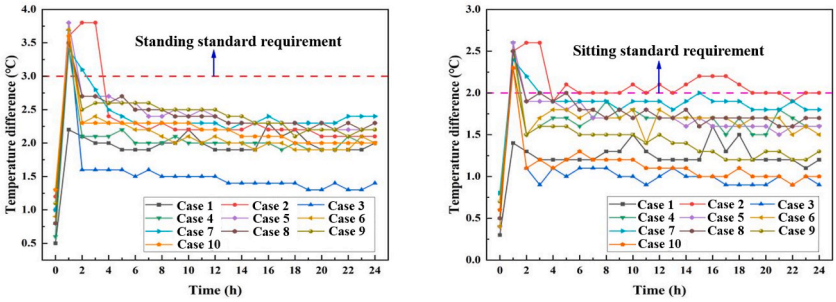

(a) Standing (b) Sitting

Fig. 11. Trend of head-to-foot temperature difference with time.

Table 4
Efficiency of waste heat emissions for 10 groups of experimental conditions.

Case	T_{in}(°C)	T_{out}(°C)	T_w(°C)	E_T
1	23.7	31.6	26.5	2.82
2	24.1	32.5	28.0	2.14
3	23.2	32.6	28.3	1.84
4	24.3	33.4	27.8	2.59
5	22.4	33.3	28.1	1.92
6	22.3	33.2	28.4	1.79
7	22.9	32.3	27.7	1.96
8	23.9	34.1	28.3	2.31
9	23.1	34.5	28.6	2.07
10	23.9	32.8	28.5	1.93

Table 5
Orthogonal test result.

Number	VR (m^3/h)	Deflector height (m)	Deflector angle (°)	Ambient temperature (°C)
1	350	1.40	0	28.7
2	350	1.25	15	29.1
3	350	1.10	30	29.4
4	300	1.40	15	29.0
5	300	1.25	30	29.2
6	300	1.10	0	29.5
7	250	1.40	30	29.0
8	250	1.25	0	29.3
9	250	1.10	15	29.7
K_1	87.2	86.7	87.5	
K_2	87.7	87.6	87.8	
K_3	88.0	88.6	87.6	
k_1	29.07	28.90	29.17	
k_2	29.23	29.20	29.27	
k_3	29.33	29.53	29.20	
Range	0.26	0.63	0.10	

temperature difference between the two conditions increases first and then decreases. At 24 h, the average ambient temperatures in the URC of case1 and case10 are 28.7 °C and 29.5 °C, respectively, with the average temperature difference is 2 °C. By reasonably arranging the deflectors, the airflow distribution inside the URC can be effectively improved, thereby enhancing the indoor temperature control performance.

4.2. Comparison of this study with other URC cooling methods

Although research on traditional cooling measures helps improve the temperature control effectiveness of the system, different cooling measures still have some limitations. Table 6 compares the energy supply methods, advantages, challenges, and application scenarios of different cooling measures for URC. Considering the existing URC, whose intake and return air layout was completed at the beginning of construction, it is difficult to improve the thermal environment of the interior spaces by modifying the ventilation mode and layout of these underground buildings. Therefore, this study proposes a mechanical ventilation with deflector cooling measure.

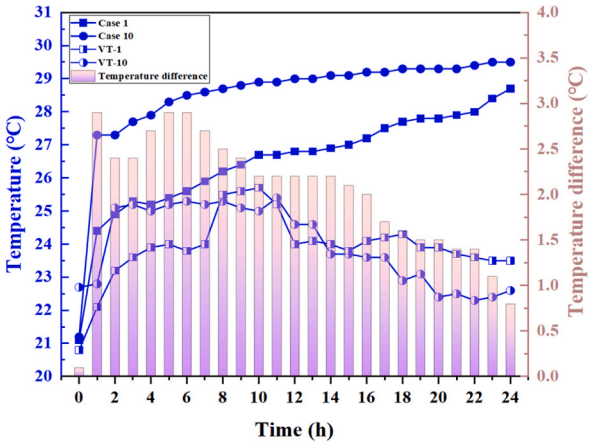

Fig. 12. Comparison of average environmental temperature changes.

Table 6
Comparison of URC cooling methods.

Cooling method	Energy supply methods	Advantages	Major challenges	Application scenarios
Natural ventilation cooling [48]	Natural convection	No electricity required, easy maintenance	Poor temperature control effect in extremely high temperatures or enclosed environments	Suitable for underground spaces with large temperature differences and favorable ventilation conditions
Ventilation cooling [49]	Passive	No safety hazards and effectively purifies air quality.	Ventilation ducts are prone to damage and rely on electricity.	Generally suitable for shallow coal mines
Ice storage cooling [50]	Passive	No safety hazards and without relying on external power	Refrigeration compressors are prone to corrosion, with high maintenance costs and ice-making costs	Any conditions
Liquid CO_2 refrigeration [51]	Passive	Not relying on external power, using phase change latent heat to carry away heat.	Prone to leakage, low in safety	Applicable to coal mines with ambient temperatures below 31 °C.
Phase change material for thermal storage [24]	Passive	Not relying on external power, excellent temperature control performance	Expensive, performance may decline after multiple phase changes	Any conditions
Mechanical ventilation with deflectors	Passive	Improve thermal environment by optimizing air flow organization, low cost, easy installation, energy saving	Deflectors are prone to damage in high temperature and high humidity environments.	Any conditions

Without changing the original ventilation method and building layout, the indoor airflow organization is optimized by rationally arranging the deflectors, thereby improving the thermal environment in the chamber.

4.3. Limitation of this study and future work

In this paper, a cooling measure of mechanical ventilation with deflectors is proposed. The distribution of air distribution can be changed by arranging deflectors to improve the thermal environment of URC. Due to the limitations of the experimental site and environmental factors, this study has the following limitations.

(1) The VT fluctuates to some extent due to the influence of ambient temperature.
(2) Due to the limitations of the experimental site, other factors such as the shape, length, and width of the deflectors on the thermal environment are not investigated.

In view of the limitations of this study, future work could focus on numerical simulations to investigate the effects of different deflector shapes, lengths, and widths under constant ventilation conditions on the thermal environment and thermal comfort in URC. By arranging different deflectors to optimize the airflow distribution inside the URC, the optimal deflector shape and arrangement can be obtained.

5. Conclusion

This paper proposes a cooling measure of mechanical ventilation with deflectors. The deflector is placed under the inlet to optimize the distribution of air flow and improve the comfort experience of evacuees. Based on the orthogonal experiment, the effects of VR, deflector height and deflector angle on the thermal environment and distribution of airflow in the URC are analyzed. A reference for the improvement of the thermal environment in underground confined spaces is provided. The main conclusions are as follows.

(1) The average temperature distribution of the URC at the three heights is: 1.8 m > 1.1 m > 0.1 m; The average temperature distribution of the front, middle and back sections is: MS > BS > FS.
(2) The ambient temperature gradient of URC decreases with the increase of VR and deflector height.
(3) The ranking of the impact of 3 factors on the ambient temperature control of the URC is as follows: deflector height > VR > deflector angle.
(4) Combined with the range analysis of orthogonal experiments and the evaluation index of airflow organization, the optimal arrangement scheme is as follows: the VR is 350 m^3/h, the deflector height is 1.40 m, and the deflector angle is 0°.
(5) Compared with the working condition without deflectors, the optimal layout can effectively reduce temperature unevenness coefficients and head-to-foot temperature difference, with an increase in waste heat emission efficiency by 46.1 % and an average decrease in ambient temperature of 2 °C.

CRediT authorship contribution statement

Hang Jin: Writing – original draft, Validation, Methodology, Investigation, Formal analysis. **Zujing Zhang:** Supervision, Resources, Methodology, Funding acquisition. **Ruiyong Mao:** Supervision, Methodology, Investigation. **Jiri Zhou:** Resources, Investigation. **Hongwei Wu:** Supervision, Resources. **Xing Liang:** Visualization, Supervision.

Declaration of competing interest

We declare that we have no financial and personal relationships with other people or organizations that can inappropriately influence our work, there is no professional or other personal interest of any nature or kind in any product, service and/or company that could be construed as influencing the position presented in, or the review of, the manuscript entitled ***'Experimental study on the optimization of thermal environment and airflow organization in a ventilated underground refuge chamber using deflectors'***.

Acknowledgments

The authors would like to thank the financial support from the National Natural Science Foundation of China (52168013), the Natural Science Foundation of Guizhou Province (ZK[2022]151) and the State Key Laboratory of Gas Disaster Detecting, Preventing and Emergency Controlling Open-fund Project (2021SKLKF10).

Data availability

Data will be made available on request.

References

[1] X. Zhang, H. Fan, F. Liu, T. Lv, L. Sun, Z. Li, W. Shang, G. Xu, Coupling coordination between the ecological environment and urbanization in the middle reaches of the yangtze river urban agglomeration, Urban Clim. 52 (2023) 101698, https://doi.org/10.1016/j.uclim.2023.101698.
[2] S. Talukdar Shahfahad, M.W. Naikoo, A. Rahman, Urban expansion and vegetation dynamics: the role of protected areas in preventing vegetation loss in a growing mega city, Habitat Int. 150 (2024) 103129, https://doi.org/10.1016/j.habitatint.2024.103129.
[3] Y. Sui, J. Hu, N. Zhang, F. Ma, Exploring the dynamic equilibrium relationship between urbanization and ecological environment – a case study of shandong province, China, Ecol. Indic. 158 (2024) 111456, https://doi.org/10.1016/j.ecolind.2023.111456.
[4] Z. Xu, S. Zhou, C. Zhang, M. Yang, M. Jiang, A bayesian network model for suitability evaluation of underground space development in urban areas: the case of changsha, China, J. Clean. Prod. 418 (2023) 138135, https://doi.org/10.1016/j.jclepro.2023.138135.
[5] H. Admiraal, A. Cornaro, Future cities, resilient cities – the role of underground space in achieving urban resilience, Undergr, Space 5 (3) (2020) 223–228, https://doi.org/10.1016/j.undsp.2019.02.001.
[6] Y. Qiao, F. Peng, Y. Luan, X. Wu, Rethinking underground land value and pricing: a sustainability perspective, Tunn. Undergr. Space Technol. 127 (2022) 104573, https://doi.org/10.1016/j.tust.2022.104573.
[7] Y. Qiao, F. Peng, X. Wu, Y. Luan, Visualization and spatial analysis of socio-environmental externalities of urban underground space use: part 2 negative externalities, Tunn. Undergr. Space Technol. 121 (2022) 104326, https://doi.org/10.1016/j.tust.2021.104326.
[8] X. Dong, Y. Wu, X. Chen, H. Li, B. Cao, X. Zhang, X. Yan, Z. Li, Y. Long, X. Li, Effect of thermal, acoustic, and lighting environment in underground space on human comfort and work efficiency: a review, Sci. Total Environ. 786 (2021) 147537, https://doi.org/10.1016/j.scitotenv.2021.147537.
[9] H. Jin, Z. Zhang, J. Zhou, R. Mao, H. Wu, X. Liang, Study on surrounding rock thermal physical properties on thermal comfort in a ventilated underground refuge chamber, Int. J. Therm. Sci. 211 (2025) 109755, https://doi.org/10.1016/j.ijthermalsci.2025.109755.
[10] X. Hu, N. Li, J. Gu, Y. He, A. Yongga, Lighting and thermal factors on human comfort, work performance, and sick building syndrome in the underground building environment, J. Build. Eng. 79 (2023) 107878, https://doi.org/10.1016/j.jobe.2023.107878.
[11] J. Yu, Y. Kang, Z.J. Zhai, Advances in research for underground buildings: energy, thermal comfort and indoor air quality, Energy Build. 215 (2020) 109916, https://doi.org/10.1016/j.enbuild.2020.109916.

[12] K. Wang, Q. Li, J. Wang, S. Yang, Thermodynamic characteristics of deep space: hot hazard control case study in 1010-m-deep mine, Case Stud. Therm. Eng. 28 (2021) 101656, https://doi.org/10.1016/j.csite.2021.101656.
[13] Y. Hu, W. Zhang, M. Wang, Y. Dong, C. Chen, Y. Zhu, D. Zhu, Research on ventilation cooling design driven by human thermal response in high geothermal temperature tunnel construction, Case Stud. Therm. Eng. 61 (2024) 104866, https://doi.org/10.1016/j.csite.2024.104866.
[14] Z. Zhang, H. Wu, K. Wang, R. Day, Y. Yuan, Air quality control in mine refuge chamber with ventilation through pressure air pipeline, Process Saf. Environ. Prot. 135 (2020) 46–58, https://doi.org/10.1016/j.psep.2019.12.014.
[15] T. Jin, Z. Zhang, L. Ge, X. Liang, H. Wu, R. Mao, Experimental investigation on thermal performance of underground refuge chamber under natural convection and ventilation, Case Stud. Therm. Eng. 52 (2023) 103637, https://doi.org/10.1016/j.csite.2023.103637.
[16] T. Jin, Z. Zhang, L. Ge, X. Liang, H. Wu, J. Zhou, R. Mao, Investigation on temperature control performance of an underground confined space under ventilation, Therm. Sci. Eng. Prog. 50 (2024) 102591, https://doi.org/10.1016/j.tsep.2024.102591.
[17] Z. Zhang, H. Wu, K. Wang, R. Day, Y. Yuan, Thermal performance of a mine refuge chamber with human body heat sources under ventilation, Appl. Therm. Eng. 162 (2019) 114243, https://doi.org/10.1016/j.applthermaleng.2019.114243.
[18] Z. Zhang, W. Guo, X. Gao, H. Wu, R. Mao, Investigation on temperature control based on cooled mine compressed air for mine refuge chamber with high-temperature surrounding rock, Int. J. Therm. Sci. 187 (2023) 108201, https://doi.org/10.1016/j.ijthermalsci.2023.108201.
[19] Z. Zhang, W. Guo, R. Mao, L. Ge, X. Liang, H. Wu, Performance analysis of an improved temperature control scheme with cold stored in surrounding rock for underground refuge chamber, Appl. Therm. Eng. 236 (2024) 121589, https://doi.org/10.1016/j.applthermaleng.2023.121589.
[20] J. Peng, J. Li, S. Zhang, G. Xing, J. Ma, B. Shang, X. Luo, Experimental and numerical investigation on a hybrid high-temperature downhole thermal management system integrating liquid cooling and phase change material, Appl. Therm. Eng. 259 (2025) 124804, https://doi.org/10.1016/j.applthermaleng.2024.124804.
[21] V.C. Midhun, S.K. Saha, Solid-solid phase change material composite based heat sink with tandem coupled heat pipe for cooling of electronics in harsh thermal environments, Appl. Therm. Eng. 267 (2025) 125846, https://doi.org/10.1016/j.applthermaleng.2025.125846.
[22] X. Li, H. Yang, R. Mao, H. Wu, X. Liang, J. Zhou, Z. Zhang, Experimental investigation on the temperature control performance of compressed air coupled phase change plate system for underground refuge chamber, Int. J. Heat Mass Tran. 233 (2024) 126028, https://doi.org/10.1016/j.ijheatmasstransfer.2024.126028.
[23] X. Gao, N. Li, Y. Xiao, Z. Zhang, M. Sun, P. Gao, Thermal storage process of phase change materials under high humidity and laminar natural convection condition: prediction model and sensitivity analysis, Energy 286 (2024) 129558, https://doi.org/10.1016/j.energy.2023.129558.
[24] X. Gao, Y. Yuan, X. Cao, H. Wu, X. Zhao, D. Yan, Coupled cooling method and application of latent heat thermal energy storage combined with pre-cooling of envelope: temperature control using phase-change chair, Sustain. Cities Soc. 42 (2018) 38–51, https://doi.org/10.1016/j.scs.2018.06.032.
[25] X. Gao, Y. Yuan, H. Wu, X. Cao, X. Zhao, Coupled cooling method and application of latent heat thermal energy storage combined with pre-cooling of envelope: optimization of pre-cooling with intermittent mode, Sustain. Cities Soc. 38 (2018) 370–381, https://doi.org/10.1016/j.scs.2018.01.014.
[26] X. Gao, Z. Zhang, Y. Yuan, X. Cao, C. Zeng, D. Yan, Coupled cooling method for multiple latent heat thermal storage devices combined with pre-cooling of envelope: model development and operation optimization, Energy 159 (2018) 508–524, https://doi.org/10.1016/j.energy.2018.06.151.
[27] W. Guo, Z. Zhang, X. Liang, H. Wu, L. Ge, R. Mao, Numerical study on the heat transfer performance of mine ice-storage cooling device, Int. J. Heat Mass Tran. 223 (2024) 125255, https://doi.org/10.1016/j.ijheatmasstransfer.2024.125255.
[28] T. Lei, T. Yang, W. Yao, J. Cao, W. Gao, Y. Li, Mechanism analysis of climate change impacts on the performance of ice storage systems, J. Energy Storage 99 (2024) 113184, https://doi.org/10.1016/j.est.2024.113184.
[29] X. Xu, S. You, X. Zheng, H. Zhang, S. Liu, Cooling performance of encapsulated ice plates used for the underground refuge chamber, Appl. Therm. Eng. 112 (2017) 259–272, https://doi.org/10.1016/j.applthermaleng.2016.10.072.
[30] Z. Zhang, W. Guo, H. Wu, L. Ge, Xing Liang, R. Mao, Thermal performance of an ice storage device for cooling compressed mine air in high-temperature mine refuge chambers, Appl. Therm. Eng. 233 (2023) 121101, https://doi.org/10.1016/j.applthermaleng.2023.121101.
[31] W. Guo, Z. Zhang, H. Wu, L. Ge, X. Liang, R. Mao, Experimental study on cooling and dehumidification performance of an ice storage air conditioner used in underground refuge chamber, Int. Commun. Heat Mass Tran. 146 (2023) 106930, https://doi.org/10.1016/j.icheatmasstransfer.2023.106930.
[32] B. Zhou, Z. Li, B. Yang, F. Wang, Z. Ai, A. Melikov, Co-flow jets application for occupant targeted ventilation: focus on thermal comfort and air quality, Build. Environ. 266 (2024) 112086, https://doi.org/10.1016/j.buildenv.2024.112086.
[33] H. Zhang, L. Wang, P. Yang, Y. Liu, C. Zhu, L. Wang, H. Zhong, Optimizing air inlet designs for enhanced natural ventilation in indoor substations: a numerical modelling and cfd simulation study, Case Stud. Therm. Eng. 59 (2024) 104408, https://doi.org/10.1016/j.csite.2024.104408.
[34] L. Wu, R. Mao, H. Wu, J. Zhang, C. Li, X. Yi, G. Huang, Z. Zhang, Optimization of airflow organization in fan-wall data center via baffles, Appl. Therm. Eng. 244 (2024) 122745, https://doi.org/10.1016/j.applthermaleng.2024.122745.
[35] R. Mao, L. Wu, Z. Zhang, H. Wu, J. Gan, J. Zhou, H. Xu, Experimental study on improving thermal management of fan-wall data center by setting baffles in cold aisle, Energy Build. 328 (2025) 115206, https://doi.org/10.1016/j.enbuild.2024.115206.
[36] Y. Xu, Z. Li, J. Wang, Y. Lu, Z. Cheng, J. Wang, Z. Lin, Improving thermal environment and ventilation efficiency in high-temperature excavation tunnels via an innovative heat insulation and cooling baffle, Therm. Sci. Eng. Prog. 55 (2024) 102992, https://doi.org/10.1016/j.tsep.2024.102992.
[37] S. Zhang, X. Huang, A. Li, B. Yu, Y. Jiang, L. Peng, Z. Chen, Improving kitchen thermal comfort in summer based on optimization of airflow distribution, J. Build. Eng. 96 (2024) 110614, https://doi.org/10.1016/j.jobe.2024.110614.
[38] C. Ren, C. Xi, J. Wang, Z. Feng, F. Nasiri, S. Cao, F. Haghighat, Mitigating covid-19 infection disease transmission in indoor environment using physical barriers, Sustain. Cities Soc. 74 (2021) 103175, https://doi.org/10.1016/j.scs.2021.103175.
[39] W. Che, J. Ding, L. Li, Airflow deflectors of external windowsto induce ventilation: towards covid-19 prevention and control, Sustain. Cities Soc. 77 (2022) 103548, https://doi.org/10.1016/j.scs.2021.103548.
[40] Z. Zhang, T. Jin, H. Wu, R. Day, X. Gao, K. Wang, R. Mao, Experimental investigation on environmental control of a 50-person mine refuge chamber, Build. Environ. 210 (2022) 108667, https://doi.org/10.1016/j.buildenv.2021.108667.
[41] H. Shao, S. Jiang, W. Tao, Z. Wu, W. Zhang, K. Wang, Theoretical and numerical simulation of critical gas supply of refuge chamber, Int. J. Min. Sci. Technol. 26 (3) (2016) 389–393, https://doi.org/10.1016/j.ijmst.2016.02.004.
[42] T. Taner, Optimisation processes of energy efficiency for a drying plant: a case of study for Turkey, Appl. Therm. Eng. 80 (2015) 247–260, https://doi.org/10.1016/j.applthermaleng.2015.01.076.
[43] Y. Zhang, J. Liu, J. Pei, J. Li, C. Wang, Performance evaluation of different air distribution systems in an aircraft cabin mockup, Aero. Sci. Technol. 70 (2017) 359–366, https://doi.org/10.1016/j.ast.2017.08.009.
[44] A. Li, Z. Liu, J. Zhang, J. Wang, Reduced-scale model study of ventilation for large space of generatrix floor in hohhot underground hydropower station, Energy Build. 43 (4) (2011) 1003–1010, https://doi.org/10.1016/j.enbuild.2010.12.026.
[45] ISO 7730:2005, Ergonomics of the Thermal Environment–Analytical Determination and Interpretation of Thermal Comfort Using Calculation of the PMV and PPD Indices and Local Thermal [S] international organization for standardization, geneva switzerland (2005).
[46] M. Krajčík, A. Simone, B.W. Olesen, Air distribution and ventilation effectiveness in an occupied room heated by warm air, Energy Build. 55 (2012) 94–101, https://doi.org/10.1016/j.enbuild.2012.08.015.
[47] K. Rhee, M. Shin, S. Choi, Thermal uniformity in an open plan room with an active chilled beam system and conventional air distribution systems, Energy Build. 93 (2015) 236–248, https://doi.org/10.1016/j.enbuild.2015.01.068.
[48] Z. Zhang, R. Day, K. Wang, H. Wu, Y. Yuan, Thermal performance analysis of an underground closed chamber with human body heat sources under natural convection, Appl. Therm. Eng. 145 (2018) 453–463, https://doi.org/10.1016/j.applthermaleng.2018.09.068.

[49] Z. Zhang, H. Wu, K. Wang, R. Day, Y. Yuan, Air quality control in mine refuge chamber with ventilation through pressure air pipeline, Process Saf. Environ. Prot. 135 (2020) 46–58, https://doi.org/10.1016/j.psep.2019.12.014.
[50] S. Wang, L. Jin, Z. Han, Y. Li, S. Ou, N. Gao, Z. Huang, Discharging performance of a forced-circulation ice thermal storage system for a permanent refuge chamber in an underground mine, Appl. Therm. Eng. 110 (2017) 703–709, https://doi.org/10.1016/j.applthermaleng.2016.08.192.
[51] Y. Junling, Y. Luwei, W. Juan, M. Yuezheng, Z. Zhentao, Study on open-cycle carbon dioxide refrigerator for movable mine refuge chamber, Appl. Therm. Eng. 52 (2) (2013) 304–312, https://doi.org/10.1016/j.applthermaleng.2012.12.014.